Astron. Astrophys. 175, 1–3 (1987)

ASTRONOMY AND ASTROPHYSICS

Deprojection of the de Vaucouleurs $r^{1/4}$ brightness profile

Y. Mellier and G. Mathez

Observatoire de Toulouse, 14, Avenue Edouard Belin, F-31400 Toulouse, France

Received July 9, accepted September 30, 1986

Summary. A tractable analytical expression is given which very closely approximates a deprojected $r^{1/4}$ brightness profile. It can be useful for a variety of applications such as numerical simulations of gravitational systems with an $r^{1/4}$ brightness profile. The method is illustrated by deducing an analytical 3D luminosity profile of the Coma cluster of galaxies.

Key words: clusters of galaxies – galaxies: structure of – analytical methods

In spite of its simple form, the de Vaucouleurs' law is well suited to fit a central intensity peak embedded in an extended halo. In particular, it fits remarkably well the brightness profile of galaxy bulges (King, 1978; Kormendy, 1977; de Vaucouleurs and Cappacioli, 1979). Moreover, the $r^{1/4}$ law can be used to fit other stellar systems such as clusters of galaxies (for example: Beers and Tonry, 1986). Pallister (1985) argued that the $r^{1/4}$ law is better than the standard isothermal King model to match clusters of galaxies density profiles since it can naturally explain the discrepancy noticed by Jones and Forman (1984) between both the so-called β_{fit} and β_{cal} (see however Gerbal et al., 1986, for another interpretation).

The physical origin of the de Vaucouleurs' law is not actually understood. Binney (1982) made an attempt to discover the distribution function hidden behind this law and found that a density profile very close to the $r^{1/4}$ law can be recovered by assuming a Boltzmann distribution function. Although no definitive conclusion has been reached yet, it seems that the de Vaucouleurs' law really reflects a scaling law which can fit galaxy bulges as well as clusters of galaxies. This indicates that the evolution mechanisms of these gravitational systems are probably quite similar. *N*-body simulations of dissipationless relaxation have shown the ability of collisionless stellar systems to reproduce density profiles very close to the de Vaucouleurs' law (Villumsen, 1984).

In a variety of simulations concerning such systems, it is often interesting to make use of an analytical density profile which has furthermore an analytical (de)projection. The so-called "modified Hubble" profile is, as far as we know, the only such example till now. Unfortunately it is not suited to all profiles and leads to divergent total mass.

Send offprint requests to: Y. Mellier

Young (1976) has numerically computed and tabulated the exact $r^{1/4}$ 3D density profile following the derivation by Poveda et al. (1960):

$$\rho(r \to 0) = r^{-3/4} \exp(-r^{1/4}) \tag{1a}$$

$$\rho(r \to \infty) = r^{-7/8} \exp(-r^{1/4})[1 - 7/8r^{-1/4} + 31/32r^{-1/2} - \ldots] \tag{1b}$$

The length unit in Eq. (1) is equal to $a = r_e/b^4$. As usual, r_e is the effective radius at half projected luminosity. b, is a numerical constant defined by the relation: $\gamma(8, b) = \Gamma(8)/2$, having the value $b = 7.66925$ (γ is the incomplete Gamma function, see for example Abramowitz and Stegun, 1964 p. 260).

To substitute a simpler expression for the above infinite series for $r \to \infty$, we tried to drop all terms but the first one, modifying it as follows:

$$\rho = r^{-\beta} \exp(-r^{\alpha}) \tag{2}$$

Due to the difference between Eqs. (1b) and (2), the best values of α and β will depend on the radius range. To determine them we made use of a code of χ^2 minimization by fitting the projection of the density in Eq. (2) to an ideal theoretical $r^{1/4}$ profile with equal error bars of arbitrary size in a logarithmic scale. From the asymptotic expansions (1a) and (1b), we first fix $\alpha = \frac{1}{4}$, checking afterwards that it is really the best value with an accuracy better than $\frac{1}{1000}$ in each of the r ranges. In Table 1 we

Table 1

$\log_{10} r/r_e$	β	χ^2	No. of bins
−5 to −3	0.963	$7\,10^{-5}$	10
−2 to −1.82	0.900	$3\,10^{-4}$	10
0.2 to 0.38	0.851	$4\,10^{-12}$	10
0.2 to 0.58	0.851	$6\,10^{-10}$	20
0.3 to 1.18	0.853	$3\,10^{-7}$	40
1.0 to 1.78	0.855	$4\,10^{-7}$	40
1.7 to 2.48	0.8576	$2\,10^{-7}$	40
2.4 to 3.18[a]	0.8547	$4\,10^{-5}$	40
3.0 to 3.39[a]	0.816	$3\,10^{-4}$	20
3.0 to 3.09	0.8595	$1\,10^{-12}$	10
2.4 to 3.18[b]	0.8516	$9\,10^{-7}$	40
−1 to 0.95[b]	0.85599	$9\,10^{-5}$	40
−2 to 2.90[b]	0.8556	$2\,10^{-3}$	50

[a] Numerical difficulties encountered in the projection

[b] The expression used for ρ was Eq. (1) with β instead of $\frac{7}{8}$

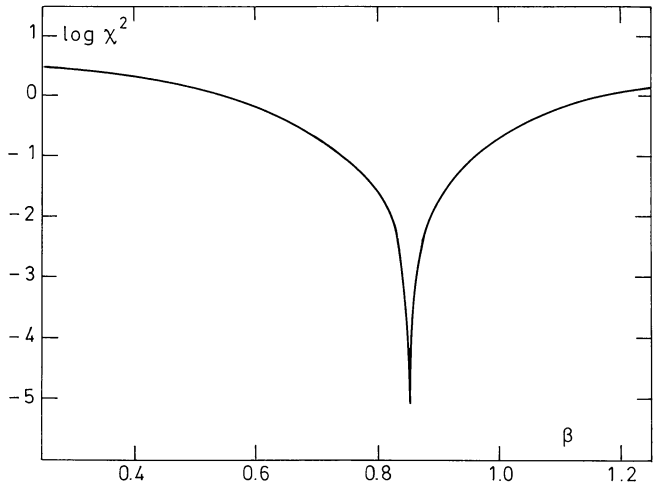

Fig. 1. The run of χ^2 between a true $r^{1/4}$ law and the projection of our approximation $\rho = r^{-\beta}e^{-r^{\alpha}}$ versus the value of β

give the best values of β corresponding to various ranges of projected radius. In a very large range, β is confined within the interval (0.853 – 0.856). Figure 1 shows the run of χ^2 versus β in the constant range $[-0.5 \leq \log r/r_e \leq 1]$.

In Table 2 the spatial density given by Young is compared to the values of ρ from Eq. (2) with $\alpha = \frac{1}{4}$ and $\beta = 0.850$, 0.855 and 0.860. All three densities are equal for $r = r_e$. $\beta = 0.855$ leads to a very good fit, although the real ρ behaves as $r^{-0.75}$ about $r \to 0$. Nevertheless, it differs by no more than 0.3 in logarithm from our expression (3) for r/r_e in the range 10^{-6} to 10^{-4}. The logarithmic difference between both spatial densities, drops from 0.10 to 0.01 for r/r_e increasing from $3\,10^{-4}$ to 0.1. Over more than 3 orders of magnitude from $r/r_e = 0.1$ to 100 the logarithmic error remains then less than 0.01. We show in Table 3 that the exact and approximate mass profiles are very similar, so that we propose the expression:

$$\rho = \rho_0 r^{-0.855} \exp(-r^{1/4}) \tag{3}$$

as a tractable approximation very close to the 3D density corresponding to the projected profile:

$$\sigma = \sigma_0 \exp(-r^{1/4}) \tag{4}$$

with $\rho_0 = \sigma_0/2a\Gamma(8)/\Gamma[(3-\beta)/\alpha]$ and $(3-\beta)/\alpha = 8.5800$.

This leads to a very simple analytical expression of the mass:

$$M(r) = M_0\gamma(8.58, r^{1/4}) \tag{5}$$

with $M_0 = 16\pi\rho_0 a^3$, so that:

$$M_{tot} = M_0\Gamma(8.58) = 1.65\,10^4\,M_0 \tag{6}$$

To check the ability of our approximate law to reproduce the spatial distribution of luminosity density in real astrophysical systems, we fit its analytical projection to the observed surface brightness profile of the Coma cluster of galaxies, determined from the data compiled by Kent and Gunn (1982). We used the 218 galaxies with $V = 3900$ to $9900\,\mathrm{km\,s^{-1}}$ in a 3° radius circle and to the limiting Zwicky magnitude $m_p = 15.7$. The results of the fit are given in Fig. 2 and Table 4. A very encouraging χ^2 probability of 97% is obtained. The expression we find for the

Table 2

r/r_e	ρ_{Young}	$\beta = 0.850$	$\beta = 0.855$	$\beta = 0.860$	$\log \rho_{0.855}/\rho_{Young}$
$1\,10^{-6}$	$2.55\,10^6$	$4.64\,10^6$	$4.97\,10^6$	$5.33\,10^6$	0.29
$3\,10^{-6}$	$1.02\,10^6$	$1.69\,10^6$	$1.81\,10^6$	$1.92\,10^6$	0.25
$1\,10^{-5}$	$3.58\,10^5$	$5.42\,10^5$	$5.75\,10^5$	$6.09\,10^5$	0.21
$3\,10^{-5}$	$1.39\,10^5$	$1.86\,10^5$	$1.96\,10^5$	$2.07\,10^5$	0.15
$1\,10^{-4}$	$4.22\,10^4$	$5.48\,10^4$	$5.74\,10^4$	$6.01\,10^4$	0.14
$3\,10^{-4}$	$1.38\,10^4$	$1.69\,10^4$	$1.76\,10^4$	$1.83\,10^4$	0.10
$1\,10^{-3}$	$3.70\,10^3$	$4.26\,10^3$	$4.41\,10^3$	$4.57\,10^3$	0.08
$3\,10^{-3}$	$9.89\,10^2$	$1.09\,10^3$	$1.12\,10^3$	$1.15\,10^3$	0.05
0.01	197	208	213	218	0.03
0.03	36.9	38.0	38.7	39.4	0.02
0.1	4.40	4.46	4.51	4.56	0.01
0.3	0.447	0.448	0.451	0.454	0.004
1.0	0.021943	0.021943	0.021943	0.021943	0
2.0	$2.847\,10^{-3}$	$2.852\,10^{-3}$	$2.843\,10^{-3}$	$2.833\,10^{-3}$	−0.0007
3.0	$7.61\,10^{-4}$	$7.64\,10^{-4}$	$7.60\,10^{-4}$	$7.55\,10^{-4}$	−0.0006
4.0	$2.80\,10^{-4}$	$2.82\,10^{-4}$	$2.80\,10^{-4}$	$2.78\,10^{-4}$	−0.0004
5.0	$1.24\,10^{-4}$	$1.25\,10^{-4}$	$1.24\,10^{-4}$	$1.23\,10^{-4}$	−0.0002
7.0	$3.40\,10^{-5}$	$3.44\,10^{-5}$	$3.40\,10^{-5}$	$3.37\,10^{-5}$	0.0004
10.	$7.82\,10^{-6}$	$7.93\,10^{-6}$	$7.84\,10^{-6}$	$7.75\,10^{-4}$	0.001
20.	$3.26\,10^{-7}$	$3.33\,10^{-7}$	$3.28\,10^{-7}$	$3.23\,10^{-7}$	0.003
30.	$4.07\,10^{-8}$	$4.18\,10^{-8}$	$4.11\,10^{-8}$	$4.04\,10^{-8}$	0.004
50.	$2.27\,10^{-9}$	$2.35\,10^{-9}$	$2.30\,10^{-9}$	$2.26\,10^{-9}$	0.006
100.	$2.63\,10^{-11}$	$2.75\,10^{-11}$	$2.69\,10^{-11}$	$2.63\,10^{-11}$	0.0098

Table 3

r/r_e	$M(r)/M_{tot}$		$1 - M(r)/M_{tot}$	
	Eq. (5)	Young	Eq. (5)	Young
$1\,10^{-6}$	$2.95\,10^{-11}$	$1.47\,10^{-11}$	1.0	1.0
$3\,10^{-6}$	$2.90\,10^{-10}$	$1.60\,10^{-10}$	1.0	1.0
$1\,10^{-5}$	$3.47\,10^{-9}$	$2.11\,10^{-9}$	0.999999997	0.999999998
$3\,10^{-5}$	$3.24\,10^{-8}$	$2.15\,10^{-8}$	0.999999968	0.999999969
$1\,10^{-4}$	$3.60\,10^{-7}$	$2.60\,10^{-7}$	0.99999964	0.99999974
$3\,10^{-4}$	$3.07\,10^{-6}$	$2.37\,10^{-6}$	0.99999693	0.99999763
$1\,10^{-3}$	$2.97\,10^{-5}$	$2.45\,10^{-5}$	0.9999703	0.9999755
$3\,10^{-3}$	$2.14\,10^{-4}$	$1.87\,10^{-4}$	0.999786	0.999813
$1\,10^{-2}$	$1.63\,10^{-3}$	$1.50\,10^{-3}$	0.99837	0.99850
$3\,10^{-2}$	$8.91\,10^{-3}$	$8.42\,10^{-3}$	0.99109	0.99158
$1\,10^{-1}$	$4.54\,10^{-2}$	$4.41\,10^{-2}$	0.9546	0.9559
$3\,10^{-1}$	0.154	0.152	0.846	0.848
1	0.416	0.415	0.584	0.585
2	0.614	0.614	0.386	0.386
3	0.724	0.725	0.276	0.275
4	0.794	0.795	0.206	0.205
5	0.841	0.842	0.159	0.158
7	0.897	0.900	0.103	0.100
10	0.942	0.943	0.058	0.057
20	0.985	0.986	0.015	0.014
30	0.994	0.995	0.006	0.005
50	0.995	0.999	0.005	0.001
100	0.9999	0.9999	0.0001	0.0001

Table 4

$\log r(')$	$\log B_{obs}$	$\log B_{0.855}$	$\log B_{1/4}$
0.79	9.36	9.37	9.37
1.22	8.89	8.89	8.88
1.50	8.44	8.50	8.49
1.68	8.22	8.21	8.21
1.84	7.99	7.93	7.93
2.00	7.67	7.62	7.62
2.16	7.21	7.28	7.28

218 galaxies, $r \leq 180'$, $m_p \leq 15.7$, $r_e = 83'$, $\chi^2 = 1.38$, $P(\chi^2) = 97\%$

luminosity inside the sphere of radius r is:

$$L(r) = 6.07\,10^8\,\gamma[8.58, (r/a)^{1/4}]\,L_0 \qquad (7)$$

$a = 0'.026$

the effective radius being then $r_e = 90'.0$.

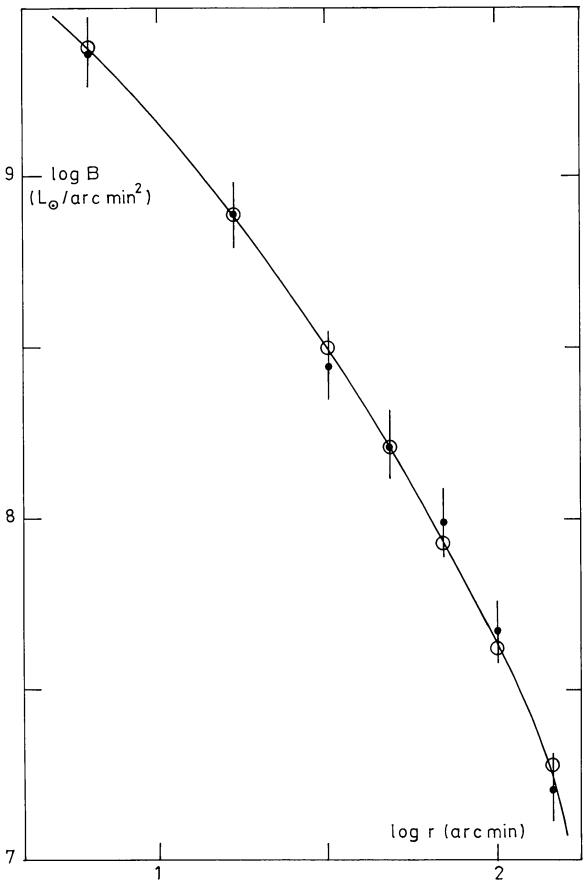

Fig. 2. The surface brightness profile of the Coma cluster of galaxies fitted by a true $r^{1/4}$ law (continuous curve) and by the projection of our approximation of the luminosity spatial density (o)

References

Abramowitz, M., Stegun, I.A.: 1964, *Handbook of Mathematical Functions*, Dover Publ. Inc., New York

Beers, T.C., Tonry, J.L.: 1986, *Astrophys. J.* **300**, 557

Binney, J.: 1982, *Monthly Notices Roy. Astron. Soc.* **200**, 951

de Vaucouleurs G., Capaccioli, M.: 1979, *Astrophys. J. Suppl.* **40**, 699

Gerbal, D., Mathez, G., Mazure, A., Salvador-Solé, E., 1986, *Astron. Astrophys.* **158**, 177

Jones, C., Forman, W., 1984, *Astrophys. J.* **276**, 38

Kent, S.M., Gunn, J., 1982, *Astron. J.* **87**, 945

King, I.R., 1978, *Astrophys. J.* **222**, 1

Kormendy, J., 1977, *Astrophys. J.* **218**, 333

Pallister, I.C., 1985, *Monthly Notices Roy. Astron. Soc.* **215**, 335

Poveda, A., Iturriaga, R., Orozco, I., 1960, *Bol. Obs. Tonantzintla y Tacubaya* **2**, 20, p. 3

Villumsen, J.V., 1984, *Astrophys. J.* **284**, 75

Young, P.J., 1976, *Astron. J.* **81**, 807